

Compact star constraints on the high-density EoS

H. Grigorian^{1,2,3}, D. Blaschke^{1,4,5} and T. Klähn^{1,6}

¹ Institut für Physik, Universität Rostock, 18051 Rostock, Germany

² Department of Physics, Yerevan State University, 375047 Yerevan, Armenia

³ Laboratory for Information Technologies, JINR Dubna, 141980 Dubna, Russia

⁴ Bogoliubov Laboratory for Theoretical Physics, JINR Dubna, 141980 Dubna, Russia

⁵ Instytut Fizyki Teoretycznej, Uniwersytet Wrocławski, 50-204 Wrocław, Poland

⁶ Gesellschaft für Schwerionenforschung mbH (GSI), 64291 Darmstadt, Germany

Abstract. A new scheme for testing the nuclear matter (NM) equation of state (EoS) at high densities using constraints from compact star (CS) phenomenology is applied to neutron stars with a core of deconfined quark matter (QM). An acceptable EoS shall not to be in conflict with the mass measurement of $2.1 \pm 0.2 M_{\odot}$ (1σ level) for PSR J0751+1807 and the mass radius relation deduced from the thermal emission of RX J1856-3754. Further constraints for the state of matter in CS interiors come from temperature-age data for young, nearby objects. The CS cooling theory shall agree not only with these data, but also with the mass distribution inferred via population synthesis models as well as with LogN-LogS data. The scheme is applied to a set of hybrid EoS with a phase transition to stiff, color superconducting QM which fulfills all above constraints and is constrained otherwise from NM saturation properties and flow data of heavy-ion collisions. We extrapolate our description to low temperatures and draw conclusions for the QCD phase diagram to be explored in heavy-ion collision experiments.

1. Introduction

Recently, new observational limits for the mass and the mass-radius relationship of CSs have been obtained which provide stringent constraints on the equation of state of strongly interacting matter at high densities, see Klähn et al. (2006) and references therein. In this latter work several modern nuclear EoS have been tested regarding their compatibility with phenomenology. It turned out that none of these nuclear EoS meets all constraints whereas every constraint could have been fulfilled by some EoS. As we will point out in this contribution, a phase transition to quark matter in the interior of CSs might resolve this problem. In the following we will apply an exemplary EoS for NM obtained from the ab-initio relativistic Dirac-Brueckner-Hartree-Fock (DBHF) approach using the Bonn A potential (van Dalen et al. 2005). There is not yet an ab-initio approach to the high-density EoS formulated in quark and gluon degrees of freedom, since

it would require an essentially nonperturbative treatment of QCD at finite chemical potentials. For some promising steps in the direction of a unified QM-NM description on the quark level, we refer to the nonrelativistic potential model approach by Röpke et al. (1986) and the NJL model one by Lawley et al. (2006). Simulations of QCD on the Lattice meet serious problems in the low-temperature finite-density domain of the QCD phase diagram relevant for CS studies. However, there are modern effective approaches to high-density QM which, albeit still simplified, focus on specific nonperturbative aspects of QCD. They differ from the traditional bag model approach and allow for CS configurations with sufficiently large masses, see Alford et al. (2006). For our QM description we employ a three-flavor chiral quark model of the NJL type with selfconsistent mean fields in the scalar meson (coupling G_S) and scalar diquark (coupling $G_D = \eta_D G_S$) channels (Blaschke et al. 2005), generalized by including a vector meson mean field (coupling $G_V = \eta_V G_S$), see Klähn et al. (2006a).

We show that the presence of a QM core in the interior of CSs does not contradict any of the discussed constraints. Moreover, CSs with a QM interior would be assigned to the fast coolers in the CS temperature-age diagram. Another interesting outcome of our investigations is the prediction of a small latent heat for the deconfinement phase transition in both, symmetric and asymmetric NM. Such a behavior leads to hybrid stars that “masquerade” as neutron stars and has been discussed earlier by Alford et al. (2005) for a different EoS. This finding is of relevance for future heavy-ion collision programs at FAIR Darmstadt.

2. The flow constraint from HICs

The behaviour of elliptic flow in heavy-ion collisions is related to the EoS of isospin symmetric matter. The upper and lower limits for the stiffness deduced from such analyses (Danielewicz et al. 2002) are indicated in Fig. 1 as a shaded region. The nuclear DBHF EoS is soft at moderate densities with a compressibility $K = 230$

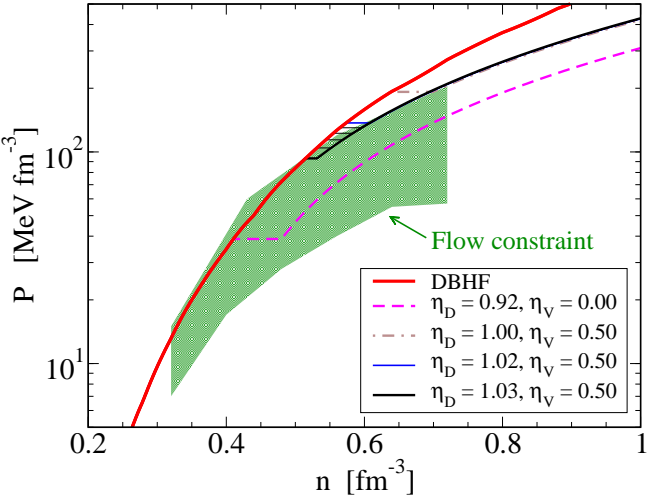


Fig. 1. Constraint on the high-density behavior of the EoS from simulations of flow data from heavy-ion collision experiments (shaded area from Danielewicz et al. 2002) compared to the nuclear matter and hybrid EoS discussed in the text.

MeV (van Dalen et al. 2004, Gross-Boelting et al. 1999), but tends to violate the flow constraint for densities above 2-3 times nuclear saturation. As a possible solution to this problem we adopt a phase transition to QM with an EoS fixed to sketch the upper boundary of the flow constraint. In order to obtain an EoS as stiff as possible we use a vector coupling of $\eta_V = 0.50$ and a diquark coupling of $\eta_D = 1.03$. Herewith the EoS is completely fixed.

3. Constraints from astrophysics

3.1. Maximum mass and mass-radius constraints

These most severe constraints come in particular from the mass measurement for PSR J0751+1807 (Nice et al. 2005) giving a lower limit for the maximum mass $\approx 1.9 M_\odot$ at 1σ level, and from the thermal emission of RX J1856-3754 (Trümper et al. 2004) providing a lower limit in the mass-radius plane with minimal radii $R > 12$ km. These constraints can only be fulfilled by a rather stiff EoS. The most stiff quark matter contribution to the EoS which still fulfills the flow constraint in symmetric matter corresponds to $\eta_V = 0.5$ with a maximum mass for hybrid stars $\approx 2.1 M_\odot$, rather independent of the choice of η_D which fixes the critical mass for the onset of deconfinement, see Figs. 2, 3. For a more detailed discussion, see Klähn et al. (2006), Klähn et al. (2006a).

3.2. Cooling constraints

Direct Urca (DU) processes are flavor-changing processes with the prototype being $n \rightarrow p + e^- + \bar{\nu}_e$ (Gamow and Schoenberg 1941), providing the most effec-

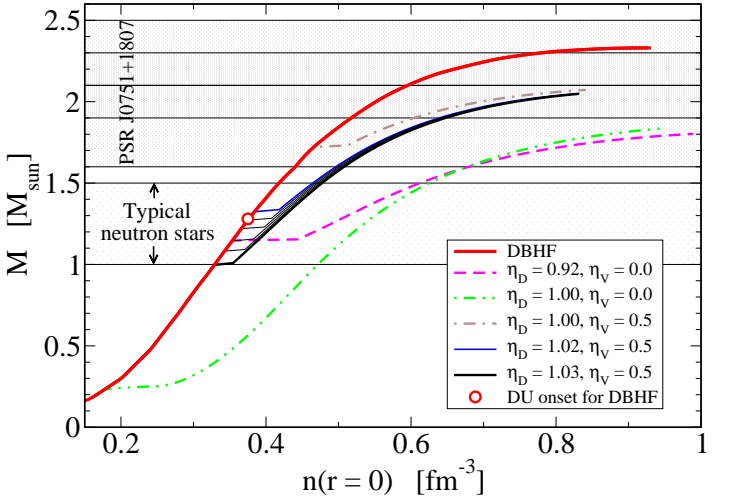


Fig. 2. Stable CS configurations for neutron stars (DBHF) and hybrid stars, characterized by the parameters η_D and η_V of the quark matter EoS.

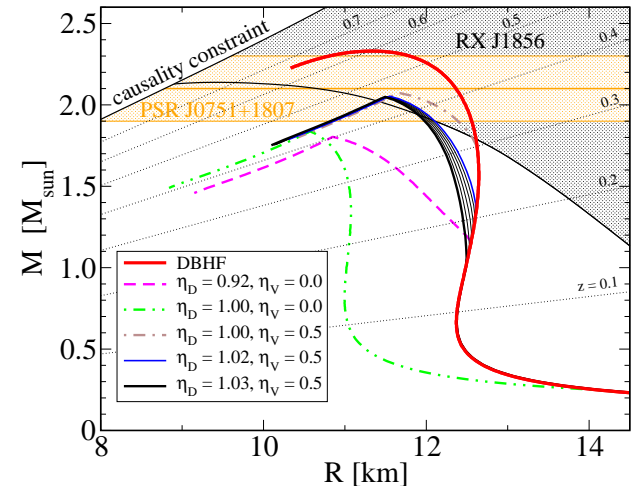


Fig. 3. Mass-radius relations for CSs with possible phase transition to deconfined quark matter, see Klähn et al. (2006a).

tive cooling mechanism in the hadronic layer of compact stars. It acts if the proton fraction x exceeds the DU threshold x_{DU} , $x = n_p/(n_n + n_p) \geq x_{DU}$. The threshold is given by $x_{DU} = 0.11$ (Lattimer et al. 1991) and rises up to $x_{DU} = 0.14$ upon inclusion of muons. Although the onset of the DU process entails a sensible dependence of cooling curves on the star masses, hadronic cooling with realistic pairing gaps is not sufficient to explain young, nearby X-ray dim objects, like Vela, with typical CS masses, not exceeding $1.5 M_\odot$ (Blaschke et al. 2004, Grigorian et al. 2005). The point on the stability curve in Fig. 2 marks the DU threshold density for the DBHF EoS. Quark matter DU processes provide en-

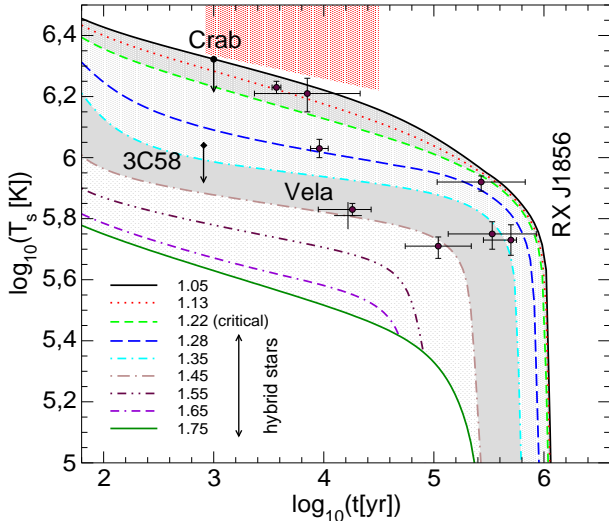


Fig. 4. Cooling evolution for hybrid stars of different masses given in units of M_{\odot} . Note that Vela is described with a typical CS mass not exceeding $1.45 M_{\odot}$. From Popov et al. 2006a.

hanced cooling, characterized by the diquark pairing gaps (Blaschke et al. 2000, Page et al. 2000) and their density dependence (Grigorian et al. 2005, Popov et al. 2006a). For a recent review, see Sedrakian (2007).

To verify this rather heuristic approach we apply explicit calculations of the cooling of hybrid configurations which shall describe present data of the *temperature-age* distribution of CSs. The main processes in nuclear matter that we accounted for are the direct Urca, the medium modified Urca and the pair breaking and formation processes. Furthermore we accounted for the $1S_0$ neutron and proton gaps and the suppression of the $3P_2$ neutron gap. For the calculation of the cooling of the quark core we incorporated the most efficient processes, namely the quark modified Urca process, the quark bremsstrahlung, the electron bremsstrahlung and the massive gluon-photon decay. In the 2-flavor superconducting phase one color of quarks remains unpaired. Here we assume a small residual pairing (Δ_X) of the hitherto unpaired quarks. For detailed discussions of cooling calculations and the required ingredients see Blaschke et al. 2004, Popov et al. 2006a, 1 and references therein. The resulting temperature-age relations for the introduced hybrid EoS are shown in Fig. 4. The critical density for the transition from nuclear to quark matter has been set to a corresponding CS mass of $M_{\text{crit}} = 1.22 M_{\odot}$. All cooling data points are covered and correspond to CS configurations with reasonable masses. In this picture slow coolers correspond to light, pure neutron stars ($M < M_{\text{crit}}$), whereas fast coolers are rather massive CSs ($M > M_{\text{crit}}$) with a QM core.

Another constraint on the temperature-age relation is given by the *maximum brightness* of CSs, as discussed by Grigorian (2006). It is based on the fact that despite many

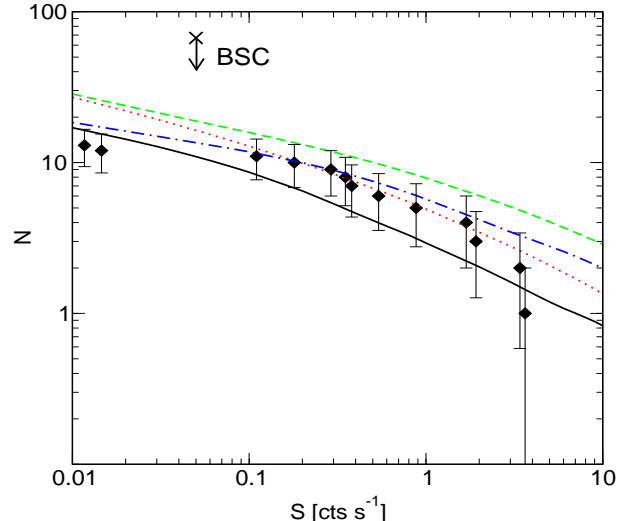


Fig. 5. Comparison of observational data for the LogN-LogS distribution with results from population synthesis using hybrid star cooling according to Popov et al. 2006a.

observational efforts one has not observed very hot NSs ($\log T > 6.3 - 6.4$ K) with ages of $10^3 - 10^{4.5}$ years. Since it would be very easy to find them - if they exist in the galaxy - one has to conclude that at least their fraction is very small. Therefore a realistic model should not predict CSs with typical masses at temperatures noticeable higher than the observed ones. The region of avoidance is the hatched trapezoidal region in Fig. 4.

The final CS cooling constraint in our scheme is given by the *Log N-Log S* distribution, where N is the number of sources with observed fluxes larger than S . This integral distribution grows towards lower fluxes and is inferred, e.g., from the ROSAT all-sky survey (Neuhäuser and Trümper 1999). The observed *Log N-Log S* distribution is compared with the ones calculated in the framework of a population synthesis approach in Fig. 5. A detailed discussion of merits and drawbacks can be found in Popov et al. (2006).

Altogether, the hybrid star cooling behavior obtained for our EoS fits all of the sketched constraints under the assumption of the existence of a 2SC phase with X-gaps.

4. Outlook: The QCD phase-diagram

Within the previous sections we exemplified how to apply the testing scheme introduced in Klähn et al. (2006) to the modeling of a reliable hybrid EoS with a NM-QM phase transition that fulfills a wide range of constraints from HICs and astrophysics. In a next step we extend the description to finite temperatures focusing on the behaviour at the transition line. For this purpose we apply a relativistic mean-field model with density-dependent masses and couplings (Typel 2005) adapted such as to mimick the DBHF-EoS and generalize to finite temper-

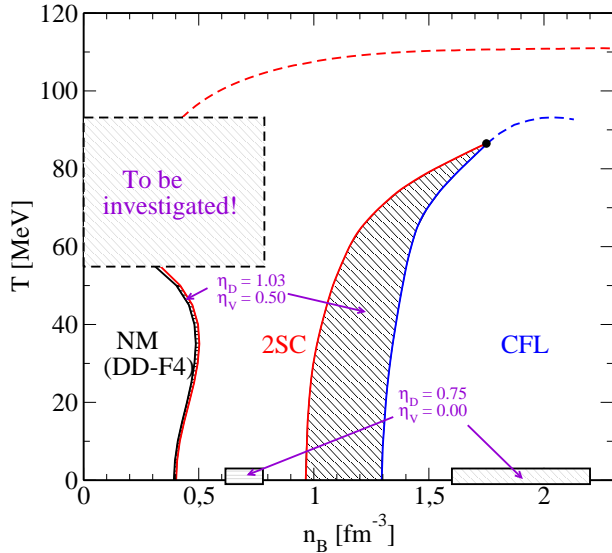


Fig. 6. Phase diagram for isospin symmetry using the most favorable hybrid EoS of the present study. The NM-2SC phase transition is almost a crossover. The model DD-F4 is used as a finite-temperature extension of DBHF. For the parameter set ($\eta_D = 0.75$, $\eta_V = 0.0$) the flow constraint is fulfilled but no stable hybrid stars are obtained.

atures (DD-F4). Fig. 6 shows the resulting phase diagram including the transition from nuclear to quark matter ($\eta_D = 1.030$, $\eta_V = 0.50$) which exhibits almost a crossover transition with a negligibly small coexistence region and a tiny density jump. At temperatures beyond $T \sim 45$ MeV our NM description is not reliable any more since contributions from mesons, hyperons and nuclear resonances are missing. This will be amended in future studies.

5. Conclusions

We have presented a new scheme for testing nuclear matter equations of state at supernuclear densities using constraints from neutron star and HIC phenomenology. Modern constraints from the mass and mass-radius-relation measurements require stiff EoS at high densities, whereas flow data from heavy-ion collisions seem to disfavor too stiff behavior of the EoS. As a compromise we have presented a hybrid EoS with a phase transition to color superconducting quark matter which, due to a vector meson meanfield, is stiff enough at high densities to allow compact stars with a mass of $2 M_\odot$. Such a hybrid EoS could be superior to a purely hadronic one as it allows a faster cooling of objects within the typical CS mass region. This way, young nearby X-ray dim objects such as Vela could be explained with masses not exceeding $1.5 M_\odot$. The present hybrid EoS predicts hybrid stars that “masquerade” as neutron stars, suggesting only a tiny density jump at the phase transition. This characteristic is also present for the symmetric matter case and persists at higher temper-

atures in the QCD phase diagram. It is suggested that the CBM experiment at FAIR might softly enter the quark matter domain without extraordinary hydrodynamical effects from the deconfinement transition.

Acknowledgements. We thank all our collaborators who have contributed to these results, in particular D. Aguilera, J. Bedermann, C. Fuchs, S. Popov, F. Sandin, S. Typel, and D.N. Voskresensky. The work is supported by DFG under grant 436 ARM 17/4/05 and by the Virtual Institute VH-VI-041 of the Helmholtz Association. We also gratefully acknowledge the support by J. E. Trümper and the organizers of the 363rd Heraeus seminar on “Neutron Stars and Pulsars”.

References

Alford M., Blaschke D., Drago A., Klähn T., Pagliara G., and Schaffner-Bielich J., 2006, arXiv:astro-ph/0606524.
 Alford M., Braby M., Paris M. W., and Reddy S., 2005, ApJ 629, 969
 Blaschke D., Klähn T. and Voskresensky D. N., 2000, ApJ 533, 406,
 Blaschke D., Grigorian H., and Voskresensky D.N., 2004, A&A 424, 979
 Blaschke D., Fredriksson S., Grigorian H., Öztas A.M. and Sandin F., 2005, PRD 72, 065020
 Blaschke D., 2006, PoS JHW2005, 003
 Danielewicz P., Lacey R., and Lynch W. G., 2002, Science 298, 1592
 Gamow G., and Schoenberg M., 1941, Phys. Rev 59, 539
 Grigorian H., Blaschke D., and Aguilera D.N., 2004, PRC 69, 065802
 Grigorian H., Blaschke D., and Voskresensky D.N., 2005, PRC 71, 045801
 Grigorian H., 2006, PRC 74, 025801
 Grigorian H., 2006a, Phys. Part. Nucl. Lett. 3, in press; arXiv:hep-ph/0602238.
 Gross-Boelting T., Fuchs C., and Faessler A., 1999, Nucl. Phys. A 648, 105
 Klähn T. et al., 2006, PRC 74, 035802
 Klähn T. et al., 2006a, arXiv:nucl-th/0609067
 Lattimer J. M. et al., 1991, Phys. Rev. Lett. 66, 2701
 Lawley S., Bentz W., and Thomas A. W., 2006, J. Phys. G 32, 667
 Neuhäuser R., and Trümper J., 1999, A&A 343, 151
 Nice D.J., et al., 2005, AJ 634, 1242
 Popov S., Grigorian H., Turolla R., and Blaschke D., 2006, A&A 448, 327
 Popov S., Grigorian H. and Blaschke D., 2006a, PRC 74, 025803
 Page D., Prakash M., Lattimer J. M., and Steiner A., PRL 85, 2048
 Röpke G., Blaschke D., and Schulz H., 1986, PRD 34, 3499.
 Sedrakian A., 2007, Prog. Part. Nucl. Phys. 58, 168
 Trümper J.E., Burwitz V., Haberl F., and Zavlin V.E., 2004, Nucl. Phys. Proc. Suppl. 132, 560
 Typel S., 2005, PRC 71, 064301
 van Dalen E.N.E., Fuchs C., and Faessler A., 2004, Nucl. Phys. A 744, 227; 2005, PRC 72, 065803
 van Dalen E.N.E., Fuchs C., and Faessler A., 2005, PRL 95, 022302